

## OPTIMIZATION OF MICRONIZING ZEOLITE GRINDING USING ARTIFICIAL NEURAL NETWORKS

V. Nikolić<sup>1#</sup>, M. Trumić<sup>1</sup>, D. Tanikić<sup>1</sup>, M. S. Trumić<sup>1</sup>

<sup>1</sup>University of Belgrade, Technical Faculty in Bor, Bor, Serbia

Received: March 20, 2024; Accepted: June 17, 2024

### Abstract

The micronizing grinding of natural zeolite, of the clinoptilolite type, was investigated in a ring mill. The aim of the experiment was to determine the optimal grinding conditions to obtain a powder with appropriate physico-chemical and microstructural characteristics that would find its potential application as a binder and ion exchanger in structural composites. The analysis of specific size classes of zeolite e after micronization was performed by grinding kinetics.

The research was carried out on previously prepared zeolite samples, on wider and narrower size classes (-3.35 + 0 mm; -3.35 + 2.36 mm; -2.36 + 1.18 mm; -1.18 + 0 mm) and different starting masses (50 g, 100 g, 200 g). Fine grinding was carried out at different time intervals (20 s, 45 s, 75 s, 120 s, 300 s, 900 s). A sieve analysis was performed on the grinding products, the content of the size class (-5 + 0)  $\mu\text{m}$  and the specific surface area of these products were determined. XRD analysis was performed on individual grinding products to take into account possible changes in the zeolite material itself. Based on the results obtained, an artificial neural network was developed and then compared with the experimental results. The artificial neural network models have achieved a satisfactory prediction accuracy (0.989 - 0.997) and can be considered accurate and very useful for the prediction of variable responses.

**Key words:** zeolite, micronizing grinding, specific surface, artificial neural networks.

### 1. Introduction

Clinoptilolite is one of the most common natural zeolites, easily obtained from mines [1], and belongs to a wide group of natural and synthetic materials that are characterized by differences in terms of their chemical, physical and structural properties [2, 3]. Natural zeolites are microporous crystals of aluminosilicate composition, a network structure composed of well-defined cavities, interconnected by channels in which cations and water molecules are located. They represent micropores of crystal hydrated aluminum silicates, and their primary or basic building block is the  $\text{TO}_4$  tetrahedron (T = Si, Al) in the center of which Si and / or Al atoms are located, while oxygen atoms are located on the forks. These units are connected in space via common oxygen atoms, building secondary polyhedral units whose connection creates a crystal (aluminosilicate) lattice.

Since the aluminosilicate lattice is formed by connecting Si(IV)-O and Al(III)-O building units, it is negatively charged, and electroneutrality is provided by cations of alkali and / or alkaline earth metals located

inside the channels and cavities of the lattice. These hydrated cations are mainly,  $\text{Na}^+$ ,  $\text{K}^+$ ,  $\text{Mg}^{2+}$  and  $\text{Ca}^{2+}$  and less frequently  $\text{Ba}^{2+}$  and  $\text{Sr}^{2+}$ . Due to weak electrostatic interactions with the aluminosilicate lattice, these cations are mobile, and in contact with the solution they are easily exchanged by ions from the solution, which gives zeolites the property of ion exchangers. Zeolites are actually forms of "molecular sieves" connected by micropores and cavities, and due to such structure and manifested ion-exchange properties, zeolites are very often used as sorbers in composite construction materials [4 - 6]. Structural voids in the range of molecular dimensions (3-10 Å) can provide space for cation reception ( $\text{Na}^+$ ,  $\text{K}^+$ ,  $\text{Mg}^+$ ,  $\text{Ba}^+$ ,  $\text{Ca}^+$ ), and various metal cations, transition metal ions (Co, Fe, Mn, Zn), as well as molecules and ions from the group ( $\text{H}_2\text{O}$ ,  $\text{NH}_3$ ,  $\text{CO}_3^{2-}$ ,  $\text{NO}_3^-$ ) [23]. Water molecules that can be reversibly desorbed are also located in channels and cavities, which gives zeolites the properties of drying agents [7, 8]. The process of micronizing grinding is intended to grind the mineral raw material to particles of micron size and thus

#Corresponding author: [vnikolic@tfbor.bg.ac.rs](mailto:vnikolic@tfbor.bg.ac.rs)

prepare it for direct application or for further technological processing. The process of micronizing grinding is mainly applied for grinding mineral raw materials that have already been crushed, by crushing and standard grinding. The application of a prolonged micronization procedure in a certain time interval under certain conditions increases the specific surface area of the treated powder, improves the reactivity and pozzolanic activity of the zeolite material, increases the cation exchange capacity and agglomerates the samples [9, 10].

Amorphization, particle size reduction, and agglomeration cause a decrease in crystallinity [11 - 13]. Micronizing grinding is performed under the action of external forces, and primarily, as with standard grinding, it is achieved by splicing surfaces, cracks and other defective places in mineral grains [14]. The main problem related to micronizing grinding at the industrial level is in the sustainability of this procedure in economic terms, so an ideal balance must be found between the achieved properties of the treated material on the one hand and the time and energy consumption for the process on the other.

Recently, artificial neural networks are increasingly used in modeling and optimizing the grinding process. Flament et al. (1993) [15, 24] in their paper considered the identification of the dynamics and reverse dynamics of a simulated grinding cycle, using neural networks. An experimental program was set up to test the management of a simulated industrial grinding cycle using a number of control strategies based on non-feedback networks [15, 24]. Ma et al. (2009) [16] developed a series of artificial neural networks (ANN) for the analysis and prediction of correlations between process parameters and morphological characteristics of nanocomposite WC-18% MgO powders using the backward error propagation algorithm (BP). The prediction results of the BP algorithm showed good coherence with the experimental data, and the optimized grinding parameters were obtained using an artificial neural network and experimental data. They came to the conclusion that the BP algorithm can be applied to grinding processes in high-energy mills [16]. Ahmadzadeh and Lundberg (2013) [17] tested different methods of predicting the wear of the lining from the mill, in the context of the remaining height and the remaining service life of the lining. They applied multiple linear regression and artificial neural networks to determine the most favorable methodology for predicting lining wear [17]. In their second paper, Ahmadzadeh

and Lundberg (2013) [18] attempted to develop a method that predicts the remaining service life of a coating, without the need to stop the mill. Artificial neural networks are designed based on various process parameters that affect the wear of the lining. The results showed an accuracy of 90%, the artificial neuron model was able to predict the remaining service life of the liner while the mill was operating; it is not necessary to stop the mill for any maintenance activity, which prevents large financial losses [18]. Singh et al. (2013) [19] developed a wrestling neural network model to predict the distribution of the granulometric composition of grinding products using available grinding data for different chromite ore grindability. They made a mathematical model that was tested on middle classes of chromite ore. The results showed a comparative accuracy of predictions for all three models, and the value of  $r^2$  varies between (0.76 - 0.93) [19]. Terzić et al. (2017) [8] examined the mechano-chemical activation of bentonite clay in an ultra-centrifugal mill, to obtain a material that is used as a binder and sorbent in building composites due to its physical-mechanical and microstructural characteristics. The activation efficiency of bentonite clay was determined by a chemometric and mathematical model of an artificial neural network. The obtained results using an artificial neural network for observing the process parameters and the quality of bentonite clay were compared with the experimental results. The value of the coefficient  $r^2$  between the experimental data and the data of the artificial neural network model for the content of the size class (- 5 + 0)  $\mu\text{m}$  is 0.811 [8]. Terzić et al. (2017) [12] in their second work examined the mechano-chemical activation of natural clinoptilolite-type zeolite from seven deposits in an ultra-centrifugal mill, for the production of powder with appropriate physicochemical and microstructural characteristics that can be used as a binder and ion exchanger in structural composites. An artificial neural network was developed on a mathematical model of the observed responses and then compared with experimental results. The artificial neural network model had 227 exit point models. Experimental results as well as the results of mathematical models showed that zeolite micronized for 30 minutes is optimal for obtaining a powder that can be used as a binder and ion exchanger. At this time of micronizing grinding, 38.8% of the content of the size class (- 5 + 0)  $\mu\text{m}$  was obtained. The value of the coefficient  $r^2$  between the experimental data and the data of the artificial neural network model for the content of the size class (- 5 + 0)  $\mu\text{m}$  is 0.936

[12]. Farizhandi et al. (2020) [20] used a planetary mill to develop a rapid assessment procedure to identify the characteristics of powders and granular materials. The grinding results in the planetary mill are then introduced into the artificial neural network model to describe the change in the distribution of the granulometric composition caused by the attrition of the particles during fluidization [20]. The modeling of an artificial neural network in this paper aims to optimize the process of micronizing grinding (in order to obtain the shortest time of micronizing grinding, the lowest energy consumption), to obtain materials with the best properties.

This paper aims to test the dry micronization of zeolite, using modern methods to determine the physico-chemical and mineralogical characteristics of micronized zeolite products, and the changes in the parameters that determine the operation of the vibrating mill with rings (grinding time, number of revolutions), as well as the analysis of the quality of the micronizing powder described by numerous parameters (specific surface area, granulometric composition for different size classes, mill filling, etc.) to obtain the finest micronized product with improved reactivity. Based on the obtained micronization results, it will be possible to predict the results using artificial neural networks to determine the best grinding conditions and the optimal product.

## 2. Experimental part

### 2.1. Materials

The paper plans to examine the dry micronization of zeolite, using modern methods for determining the physicochemical and mineralogical characteristics of micronized zeolite products, and changes in parameters that determine the operation of the vibrating mill with rings (grinding time, number of revolutions), as well as quality analysis of micronizing powder. Numerous parameters (specific surface, granulometric composition for different size classes, mill filling, etc.), in order to obtain the finest micronized product of improved reactivity. Based on the obtained results of micronizing grinding, the results will be predicted using artificial neural networks, in order to determine the best grinding conditions and the optimal product.

The zeolite sample is gray, while the crystals are lithocrystalloclastic to crystalloclastic. It contains about 90% zeolite, in a smaller amount quartz, feldspar, mica and calcite and traces of illite. Prior to the micronization

grinding process, sample preparation was carried out. The zeolite sample was first crushed in a laboratory jaw crusher to an upper limit size of 3.35 mm. This was followed by homogenization, splitting of the sample and representative sampling. Four size fractions (- 3.35 + 0 mm; - 3.35 + 2.36 mm; - 2.36 + 1.18 mm; - 1.18 + 0 mm) in different starting masses (50 g, 100 g, 200 g) were also prepared and subjected to micronizing grinding. Chemical analysis of the zeolite sample was determined by a standard analytical method. The results of the chemical analysis are given in Table 1 [14].

**Table 1** Chemical composition of the initial zeolite sample [14]

Component	SiO <sub>2</sub>	Al <sub>2</sub> O <sub>3</sub>	Fe <sub>2</sub> O <sub>3</sub>	CaO	MgO	K <sub>2</sub> O	Na <sub>2</sub> O	LoI*
Content, %	64.05	15.29	2.52	4.82	1.33	0.77	1.27	9.86

\* LoI - Loss on ignition determined as weight difference between 20 ° and 1000 °C

### 2.2. Micronizing grinding

Micronizing grinding of zeolite was performed in a laboratory vibrating mill with rings of the type "SIEBTECHNIK TS-250", at a speed of 1000 rpm in a time interval of 20 s, 45 s, 75 s, 120 s, 300 s, and 900 seconds. The content of the size class (- 5 + 0) μm, which was determined using ultrasonic sieve (US1-RETSCH), and the theoretical specific surface area were monitored.

### 2.3. Mineralogical characteristics of zeolites

X - ray diffraction analysis was performed on characteristic samples of grinding products. X ray diffraction analysis was used to determine and monitor the phase composition of the samples. The samples were analyzed on an X-ray diffractometer of the "PHILIPS" brand, model PW-1710 with a curved graphite monochromator and a scintillation counter. The intensities of diffracted CuKα ray radiation (λ=1.54178Å) were measured at room temperature in the intervals of 0.02 °2θ and time from 1 and in the range from 4 to 65 °2θ. The X-ray tube was loaded with a voltage of 40 kV and a current of 30 mA, while the slots for directing the primary and diffracted beam 1° and 0.1 mm [14].

### 2.4. Modeling of artificial neural networks

In this research, models based on the Multi Layer

Perceptron were used, which in principle consist of three layers (input layer, hidden layer and output layer). The first estimation of the neuron number was obtained from a number of input and output neurons, the number of neurons in the hidden layer and number of weights (connections between layers) in the neural network. Number of neurons in a hidden layer depends on the complexity of the relationship between inputs and outputs. In this study, the number of hidden neurons in the ANN model varied from  $n=4$  to 10. There were  $x=3$  inputs,  $y=15$  outputs, and  $m=81-210$  wt coefficients (depending on  $n$ ). Binary step was used in the activation function. The learning rate was 0.1.

The optimum number of hidden neurons was chosen upon minimizing the difference between predicted ANN values and desired outputs, using  $r^2$  during testing as a performance indicator. The coefficient of determination ( $r^2$ ) is compared below with

the values obtained by other researchers.

It is also the most commonly used and most flexible model of an artificial neural network of general purpose. The input values of this model were size class, grinding time and initial mass of the sample, while the output values were the content of the size class ( $-5 + 0$ )  $\mu\text{m}$  and the specific area. An artificial neural network with feed forward error backpropagation was used in the paper. The network "learns" using the Levenberg-Marquardt algorithm due to its high accuracy [12, 25].

### 3. Results and discussion

The increase in the time of micronizing grinding led to a change in the characteristics of zeolite and the manifestation of differences between unground and ground zeolite. The results of micronizing grinding are shown in Tables 2-5.

**Table 2** Content of the size class ( $-5 + 0$ )  $\mu\text{m}$  of the sample ( $-3.35 + 0$ ) mm, after micronizing grinding, starting masses (50, 100 and 200) g [14, 26]

50 g						
Time	20 s	45 s	75 s	120 s	300 s	900 s
Size class ( $\mu\text{m}$ )	-5 + 0	-5 + 0	-5 + 0	-5 + 0	-5 + 0	-5 + 0
W (%)	95.90	97.40	95.86	94.08	81.04	80.18
Spec. surface area ( $\text{m}^2/\text{kg}$ )	1056.02	1070.77	1056.65	1036.41	895.96	888.22
100 g						
Time	20 s	45 s	75 s	120 s	300 s	900 s
Size class ( $\mu\text{m}$ )	-5 + 0	-5 + 0	-5 + 0	-5 + 0	-5 + 0	-5 + 0
W (%)	90.98	94.15	95.83	94.31	82.11	64.99
Spec. surface area ( $\text{m}^2/\text{kg}$ )	1006.26	1039.44	1055.46	1038.20	908.23	723.16
200 g						
Time	20 s	45 s	75 s	120 s	300 s	900 s
Size class ( $\mu\text{m}$ )	-5 + 0	-5 + 0	-5 + 0	-5 + 0	-5 + 0	-5 + 0
W (%)	83.22	92.49	93.48	93.39	90.76	71.49
Spec. surface area ( $\text{m}^2/\text{kg}$ )	922.29	1020.16	1031.95	1031.64	1001.81	797.52

**Table 3** Content of size class ( $-5 + 0$ )  $\mu\text{m}$  of sample ( $-3.35 + 2.36$ ) mm, after micronizing grinding, starting masses (50, 100 and 200) g [14, 26]

50 g						
Time	20 s	45 s	75 s	120 s	300 s	900 s
Size class ( $\mu\text{m}$ )	-5 + 0	-5 + 0	-5 + 0	-5 + 0	-5 + 0	-5 + 0
W (%)	93.03	95.71	94.63	91.64	81.03	76.78
Spec. surface area ( $\text{m}^2/\text{kg}$ )	1027.67	1053.86	1042.69	1012.06	897.11	852.43
100 g						
Time	20 s	45 s	75 s	120 s	300 s	900 s
Size class ( $\mu\text{m}$ )	-5 + 0	-5 + 0	-5 + 0	-5 + 0	-5 + 0	-5 + 0
W (%)	89.92	94.83	95.34	94.78	86.63	74.49
Spec. surface area ( $\text{m}^2/\text{kg}$ )	996.46	1046.60	1050.40	1045.26	957.48	826.11
200 g						
Time	20 s	45 s	75 s	120 s	300 s	900 s
Size class ( $\mu\text{m}$ )	-5 + 0	-5 + 0	-5 + 0	-5 + 0	-5 + 0	-5 + 0
W (%)	77.75	90.72	93.01	95.33	92.97	76.82
Spec. surface area ( $\text{m}^2/\text{kg}$ )	864.01	1002.84	1027.77	1050.04	1024.66	849.60

**Table 4** Content of size class (- 5 + 0)  $\mu\text{m}$  of sample (- 2.36 + 1.18) mm, after micronizing grinding, initial masses (50, 100 and 200) g [14, 26]

50 g						
Time	20 s	45 s	75 s	120 s	300 s	900 s
Size class ( $\mu\text{m}$ )	- 5 + 0	- 5 + 0	- 5 + 0	- 5 + 0	- 5 + 0	- 5 + 0
W (%)	94.12	96.53	96.37	93.04	85.80	79.29
Spec. surface area ( $\text{m}^2/\text{kg}$ )	1039.29	1062.18	1060.31	1026.50	946.92	878.86
100 g						
Time	20 s	45 s	75 s	120 s	300 s	900 s
Size class ( $\mu\text{m}$ )	- 5 + 0	- 5 + 0	- 5 + 0	- 5 + 0	- 5 + 0	- 5 + 0
W (%)	93.44	93.62	93.94	93.83	84.54	70.48
Spec. surface area ( $\text{m}^2/\text{kg}$ )	1029.96	1035.05	1037.55	1036.92	935.84	784.92
200 g						
Time	20 s	45 s	75 s	120 s	300 s	900 s
Size class ( $\mu\text{m}$ )	- 5 + 0	- 5 + 0	- 5 + 0	- 5 + 0	- 5 + 0	- 5 + 0
W (%)	81.80	92.42	95.61	95.69	93.65	75.18
Spec. surface area ( $\text{m}^2/\text{kg}$ )	906.09	1019.29	1054.08	1054.56	1032.70	833.96

**Table 5** Content of size class (- 5 + 0)  $\mu\text{m}$  of sample (- 1.18 + 0) mm, after micronizing grinding, starting masses (50, 100 and 200) g [14, 26]

50 g						
Time	20 s	45 s	75 s	120 s	300 s	900 s
Size class ( $\mu\text{m}$ )	- 5 + 0	- 5 + 0	- 5 + 0	- 5 + 0	- 5 + 0	- 5 + 0
W (%)	96.28	96.15	92.75	91.72	86.98	82.84
Spec. surface area ( $\text{m}^2/\text{kg}$ )	1059.86	1058.75	1026.59	1015.20	961.18	919.22
100 g						
Time	20 s	45 s	75 s	120 s	300 s	900 s
Size class ( $\mu\text{m}$ )	- 5 + 0	- 5 + 0	- 5 + 0	- 5 + 0	- 5 + 0	- 5 + 0
W (%)	92.87	94.50	95.20	94.16	88.86	66.78
Spec. surface area ( $\text{m}^2/\text{kg}$ )	1025.54	1042.88	1049.27	1038.06	980.73	745.39
200 g						
Time	20 s	45 s	75 s	120 s	300 s	900 s
Size class ( $\mu\text{m}$ )	- 5 + 0	- 5 + 0	- 5 + 0	- 5 + 0	- 5 + 0	- 5 + 0
W (%)	82.41	92.72	94.37	93.87	90.60	76.17
Spec. surface area ( $\text{m}^2/\text{kg}$ )	912.77	1023.59	1040.74	1036.79	1001.55	844.26

As the time of micronized grinding increases, the content of the class (- 5 + 0)  $\mu\text{m}$  [12] and the specific surface area [12] increase until a certain grinding time, and after that it is assumed that agglomeration of samples occurs. For all samples, the optimal grinding time is between (45 and 75) seconds, during which time the sample is ground and the specific surface area is increased. At longer grinding times the specific surface area is reduced as the agglomeration process is assumed to take place. The content of the size class (- 5 + 0)  $\mu\text{m}$  increases to 95%, and then it reduces as grinding time increases. In order to determine whether agglomeration occurred, X-ray diffraction analysis was performed on a sample of class (- 3.35 + 0) mm with a starting mass of 50 g.

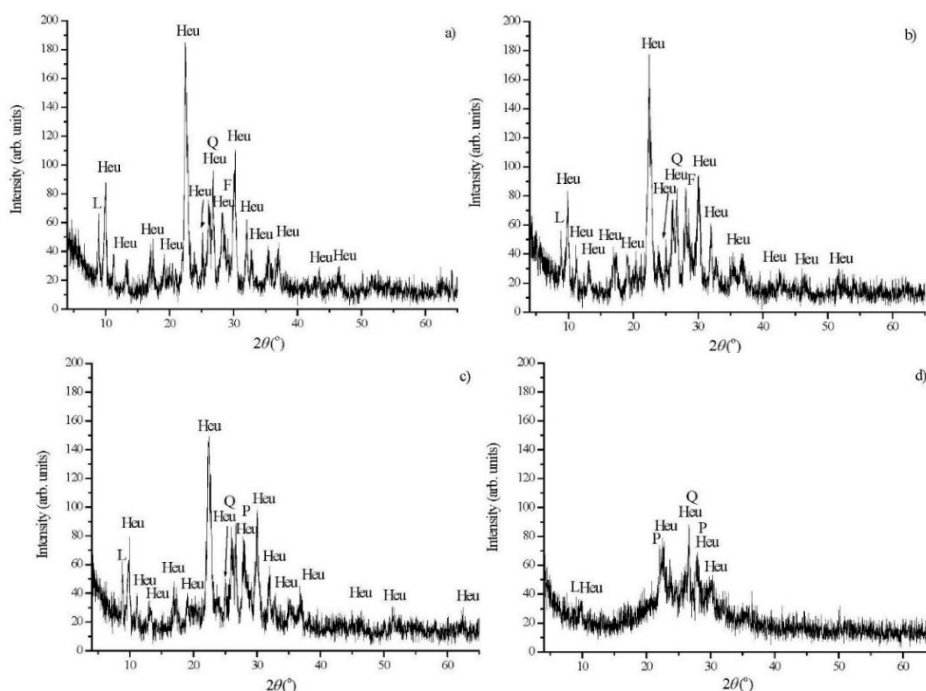
### 3.1. X-ray diffraction analysis

Figure 1 shows a comparative representation of the diffractogram of the unground sample and the sample with a starting weight of 50 g micronized (45, 120 and 900) seconds [14].

All samples were examined by X - ray diffraction on a polycrystalline sample. The mineral composition of the unground sample (Figure 1 a)) is as follows: HEU type minerals, quartz, feldspar, mica, and the most common is zeolite minerals, while quartz, feldspars and mica are significantly less represented. Of the feldspar, plagioclase is more predominantly represented than K-feldspar, and of the carbonate mineral, the presence of trace calcite was found. In the micronized sample for 45 seconds (Figure 1 b)), the content of zeolite minerals did

not decrease compared to the unground sample, and the effects of amorphization due to grinding were not seen [12]. In the sample shown in Figure 1 c), the content of zeolite minerals begins to decrease, and the effects of amorphization due to grinding are weak, while in the sample in Figure 1 d) the effects of amorphization due to grinding are very pronounced, and zeolite

minerals in the crystalline they are practically in shape [12], i.e. most of them are amorphized [8]. The authors [11, 12, 21, 22] also confirmed that agglomerations of zeolites occur after micronizing grinding. In order to see whether the obtained results can be tested and whether the results can be predicted, a neural network modeling was performed in the Matlab program.



**Figure 1** XRD analysis of unground sample (a) and sample with starting weight of (50 g) micronized: b) 45 sec; c) 120 sec; d) 900 sec [14]

### 3.2. Zeolite micronizing grinding modeling

The inputs of the models were size classes (-3.35 + 0 mm; -3.35 + 2.36 mm; -2.36 + 1.18 mm; -1.18 + 0 mm), grinding time (20 s, 45 s, 75 s, 120 s, 300 s, 900 s) and the initial mass of the sample (50 g, 100 g, 200 g), while the output values were content of the size class (- 5 + 0)  $\mu\text{m}$  and specific area. The results from Tables 2-5 were inserted into the Multi Layer Perceptron model and tested. The database used for modeling artificial neural networks in Matlab was divided into three sets: a network training set (70%), a validation set (15%) and a testing set (15%). A cross-validation data set was used to test network performance, while a data set used during the training was used as an indicator of the level of generalization and an indicator of the time when the network completed the training [12]. A set of test data

was used to examine the possibility of network generalization. Testing of the model showed that the network achieves good results, which is shown in Figure 2, having in mind a small set of input-output data. The accuracy of the results is confirmed by a very large coefficient  $R$  that ranges (0.989 - 0.997), which gives a satisfactory prediction accuracy. Comparing the obtained results with the results of other authors [8, 12], who for a much larger number of input-output data obtained that the value of the coefficient  $r^2$  between experimental data and artificial neural network model data for size class content (- 5 + 0)  $\mu\text{m}$  is 0.811 for bentonite [8] and 0.936 for zeolite [12], it can be concluded that this model gave very good results, considering the much smaller the number of input-output data in relation to the authors [8, 12], and this statement is confirmed

by the moving coefficient  $R$  (0.989 - 0.997).

Figures 3 and 4 show a comparison of the calculated

values compared with the experimental data for the optimal artificial neural network.

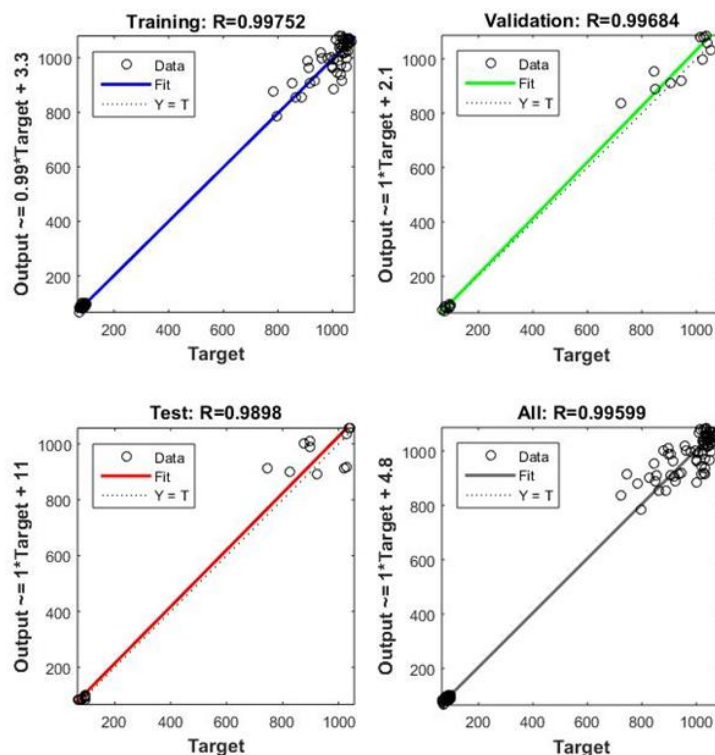


Figure 2 Experimentally obtained values of parameters and values obtained using the ANN model [26]

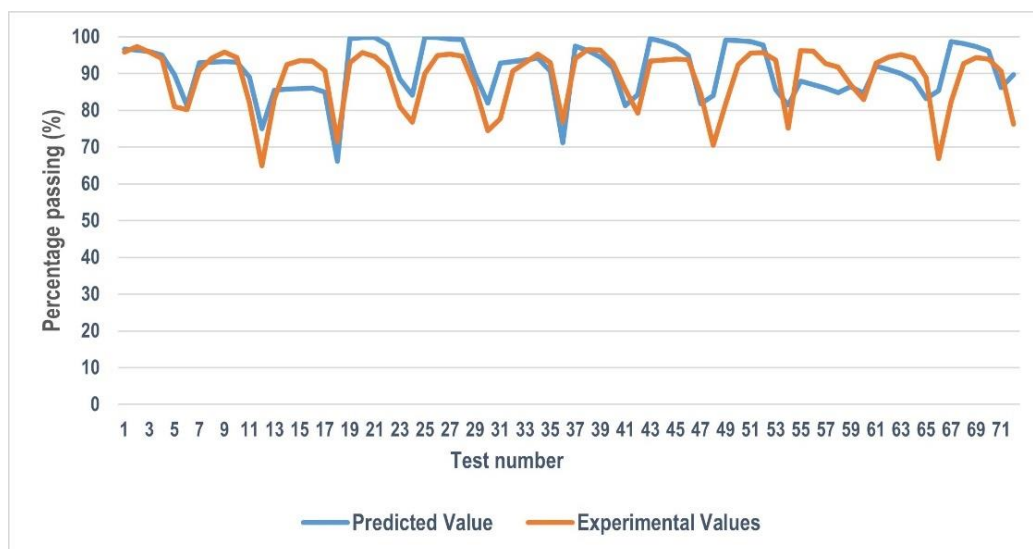


Figure 3 Comparative values of the content of the class (- 5 + 0)  $\mu\text{m}$  obtained experimentally and using the ANN model [26]



**Figure 4** Comparative values of specific surface obtained experimentally and using the ANN model [26]

From diagrams 3 and 4 it can be seen that the modeling of the network is well done, the neural network has well captured the trend of change of curves obtained on the basis of experimental results. It was calculated that the mean error of the obtained model for the content of the size class  $(- 5 + 0) \mu\text{m}$  is about 6%, and for a specific area about 4.5%, which is considered a very good prediction.

#### 4. Conclusion

Micronizing grinding is a complex, long and complicated process, but the possibility of using neural networks as a tool for predicting results in such research facilitates and speeds up the work, and enables more accurate results. The study presents a comprehensive approach of artificial neural networks that can predict the content of the size class  $(- 5 + 0) \mu\text{m}$  and the specific surface with great certainty. Neural networks are applied to this grinding process because neural networks rely less on an accurate physical model, and are mostly based on a statistic approach. Therefore, neural networks can be ideal for modeling this complex grinding process, which is the correlation coefficient and confirmed by its predictive accuracy that ranges (0.989 - 0.997). The mean error obtained for both models does not exceed 6%, which tells us that the model performed a very good prediction of the results.

#### Note

A part of this study was presented at the XV International Mineral Processing and Recycling Conference, organized by the University of Belgrade, Technical Faculty in Bor, from 17-19 May 2023, Belgrade, Serbia.

#### Acknowledgements

"The research presented in this paper was done with the financial support of the Ministry of Science, Technological Development and Innovation of the Republic of Serbia, within the funding of the scientific research work at the University of Belgrade, Technical Faculty in Bor, according to the contract with registration number 451-03-65/2024-03/200131".

#### 5. References

- [1] Mansouri, N., Rikhtegar, N., Panahi, A.H., Atabi, F., Shahraki, K.B. (2013) Porosity, characterization and structural properties of natural zeolite-clinoptilolite - as a sorbent. *Environment Protection Engineering*, 39 (01), 139-152.
- [2] Liebau, F. (1983) Zeolites and clathrasils - Two distinct classes of framework silicates. *Zeolites*, 3 (3), 191-193.



- [3] Auerbach, S.M., Carrado, K.A., Dutta, P.K. (2003) Handbook of Zeolite Science and Technology. 1<sup>st</sup> edition, CRC Press, New York & Basel.
- [4] Kusuma, R., Hadinoto, J., Ayucitra, A., Soetaredjo, F., Ismadji, S. (2013) Natural zeolite from Pacitan Indonesia, as catalyst support for transesterification of palm oil. *Applied Clay Science*, 74, 121-126.
- [5] Rida, K., Bouraoui, S., Hadnine, S. (2013) Adsorption of methylene blue from aqueous solution by kaolin and zeolite. *Applied Clay Science*, 83-84, 99-105.
- [6] Musyoka, N., Missengue, R., Kuisakana, M., Petrik, L. (2014) Conversion of South African clays into high quality zeolites. *Applied Clay Science*, 97-98, 182-186.
- [7] Alver, B., Sakizci, M., Yörükoğullari, E. (2010) Investigation of clinoptilolite rich natural zeolites from Turkey: a combined XRF, TG/DTG, DTA and DSC study. *Journal of Thermal Analysis and Calorimetry*, 100 (1), 19-26.
- [8] Terzić, A., Pezo, L., Andrić, L., Pavlović, V.B., Mitić, V.V. (2017) Optimization of bentonite clay mechano-chemical activation using artificial neural network modeling. *Ceramics International*, 43 (2), 2549-2562.
- [9] Kang, S.J., Egashira, K. (1997) Modification of different grades of Korean natural zeolites for increasing cation exchange capacity. *Applied Clay Science*, 12 (1-2), 131-144.
- [10] Villa, C., Pecina, E.T., Torres, R., Gómez, L. (2010) Geopolymer synthesis using alkaline activation of natural zeolite. *Construction and Building Materials*, 24 (11), 2084-2090.
- [11] Tunç, T., Demirkıran, A.Ş. (2014) The effects of mechanical activation on the sintering and microstructural properties of cordierite produced from natural zeolite. *Powder Technology*, 260, 7-14.
- [12] Terzić, A., Pezo, L., Andrić, L. (2017) Chemometric assessment of mechano-chemically activated zeolites for application in the construction composites. *Composites Part B: Engineering*, 109, 30-44.
- [13] Bohács, K., Kristály, F., Mucsi, G. (2018) The influence of mechanical activation on the nanostructure of zeolite. *Journal of Materials Science*, 53 (19), 13779-13789.
- [14] Andrić Lj., Trumić, M., Trumić, M., Nikolić, V. (2018) Micronization of zeolite in vibration mill. *Recycling and Sustainable Development*, 11, 63-71.
- [15] Flament, F., Thibault, J., Hodouin, D. (1993) Neural network based control of mineral grinding plants. *Minerals Engineering*, 6 (3), 235-249.
- [16] Ma, J., Zhu, S.G., Wu, C.X., Zhang, M.L. (2009). Application of back-propagation neural network technique to high-energy planetary ball milling process for synthesizing nanocomposite WC–MgO powders. *Materials & Design*, 30 (8), 2867-2874.
- [17] Ahmadzadeh, F., Lundberg, J. (2013) Application of multi regressive linear model and neural network for wear prediction of grinding mill liners. *International Journal of Advanced Computer Science and Applications*, 4 (5), 53-58.
- [18] Ahmadzadeh, F., Lundberg, J. (2013) Remaining useful life prediction of grinding mill liners using an artificial neural network. *Minerals Engineering*, 53, 1-8.
- [19] Singh, V., Banerjee, P.K., Tripathy, S.K., Saxena, V.K., Venugopal, R. (2013) Artificial neural network modeling of ball mill grinding process. *Journal of Powder Metallurgy & Mining*, 2 (2), 1-4.
- [20] Farizhandi, A.A.K., Zhao, H., Chen, T., Lau, R. (2020) Evaluation of material properties using planetary ball milling for modeling the change of particle size distribution in a gas-solid fluidized bed using a hybrid artificial neural network-genetic algorithm approach. *Chemical Engineering Science*, 215, 1-20.
- [21] Zolzaya, T., Davaabal, B., Ochirbat, Z., Oyun-Erdene, G., Minjigmaa, A., Temuujiin, J. (2011) The mechanochemical activation study of Tsagaan-tsav zeolite. *Mongolian Journal of Chemistry*, 12 (38), 98-101.
- [22] Qiu, W., Vakili, M., Cagnetta, G., Huang, J., Yu, G. (2020) Effect of high energy ball milling on organic pollutant adsorption properties of chitosan. *International Journal of Biological Macromolecules*, 148, 543-549.
- [23] Alver, B., Sakizci, M., & Yörükoğullari, E. (2010) Investigation of clinoptilolite rich natural zeolites from Turkey: a combined XRF, TG/DTG, DTA and DSC study. *Journal of Thermal Analysis and Calorimetry*, 100 (1), 19-26.
- [24] Thibault, J., Flament, F., Hodouin, D. (1992) Modelling and control of mineral processing plants using neural networks. *IFAC Proceedings Volumes*, 25 (17), 25-30.

- [25] Suri, N.R., Deodhare, D., Nagabhushan, P. (2002) Parallel Levenberg-Marquardt-Based Neural Network Training on Linux Clusters-A Case Study. In: Third Indian Conference on Computer Vision, Graphics & Image Processing. Ahmadabad, India, Proceedings, 1-6.
- [26] Nikolić V., Trumić M., Tanikić D. (2023) Optimization of micronizing zeolite grinding using artificial neural networks. In: XV International Mineral Processing and Recycling Conference. Belgrade, Serbia, Proceedings, 143-149.

## OPTIMIZACIJA MIKRONIZACIJE MLEVENJA ZEOLITA KORIŠĆENJEM VEŠTAČKIH NEURONSKIH MREŽA

V. Nikolić<sup>1#</sup>, M. Trumić<sup>1</sup>, D. Tanikić<sup>1</sup>, M. S. Trumić<sup>1</sup>

<sup>1</sup>Univerzitet u Beogradu, Tehnički fakultet u Boru, Bor, Srbija

Primljen: 20. marta 2024.; Prihvaćen: 17. juna 2024.

### Izvod

Mikronizirajuće mlevenje prirodnog zeolita, tipa klinoptilolit, ispitivano je u prstenastom mlinu. Cilj eksperimenta je bio da se odrede optimalni uslovi mlevenja za dobijanje praha sa odgovarajućim fizičko-hemijskim i mikrostrukturnim karakteristikama koji bi našao svoju potencijalnu primenu kao vezivo i jonski izmjenjivač u konstrukcionim kompozitima. Analiza određenih klasa krupnoće zeolita nakon mikronizacije izvršena je preko kinetike mlevenja. Istraživanja su vršena na prethodno pripremljenim uzorcima zeolita, na širim i užim klasama krupnoće (-3,35 + 0 mm; -3,35 + 2,36 mm; -2,36 + 1,18 mm; -1,18+0 mm) i različitim polaznim masama (50 g, 100 g, 200 g). Fino mlevenje je vršeno u različitim vremenskim intervalima (20 s, 45 s, 75 s, 120 s, 300 s, 900 s). Na proizvodima mlevenja izvršena je sitovna analiza, određen je sadržaj klase krupnoće (-5+0)  $\mu\text{m}$  i specifična površina ovih proizvoda. Na pojedinim proizvodima mlevenja izvršena je XRD analiza u cilju sagledavanja potencijalnih promena u samom materijalu-zeolitu. Veštačka neuronska mreža je razvijena na osnovu dobijenih rezultata, koja je nakon toga upoređena sa dobijenim eksperimentalnim rezultatima. Modeli veštačke neuronske mreže izvršili su zadovoljavajuću tačnost predviđanja (0,989 - 0,997) i mogu se smatrati preciznim i vrlo korisnim za predviđanje promenljivih odziva.

**Ključne reči:** zeolit, mikronizirajuće mlevenje, specifična površina, veštačke neuronske mreže.